# Comprehensive Evaluation of Patients with Suspected Renal Hypertension Using MDCT: From Protocol to Interpretation

I-Chen Tsai[1, 2]
Min-Chi Chen[1,3]
Wen-Lieng Lee[2,4]
Pao-Chun Lin[1,3]
I-Tzun Tsai[5]
Wan-Chun Liao[1,3]
Clayton Chi-Chang Chen[1,3]

**OBJECTIVE.** The objectives of this article are to, first, describe the reasons for and details of the MDCT protocol for patients with suspected renal hypertension; second, explain the importance of comprehensive evaluation by MDCT in patients with suspected renal hypertension; third, review the image appearances of important conditions that may be encountered in the reader's clinical practice; and, fourth, explain what information should be included in a comprehensive MDCT report for patients with suspected renal hypertension.

**CONCLUSION.** MDCT is widely used for renal artery evaluation in patients with resistant hypertension. Because the regions outside the renal arteries might also have diseases that contribute to the symptoms, a comprehensive interpretation including the renal arteries, renal parenchyma, adrenal glands, and scanned abdomen is very important. The scanning parameters should be adjusted according to the patient's body habitus because some patients with suspected renal hypertension are children or young women. In this article, cases with illustrations showing the process from protocol to interpretation are provided.

**Keywords:** abdominal imaging, adrenal glands, CT, kidneys, radiation dose, renal artery stenosis, renal hypertension

DOI:10.2214/AJR.08.1355

Received June 5, 2008; accepted after revision September 15, 2008.

[1]Department of Radiology, Taichung Veterans General Hospital, No. 160, Sec. 3, Taichung Harbor Rd., Taichung 407, Taiwan, ROC. Address correspondence to I. C. Tsai (sillyduck.radiology@gmail.com).

[2]Institute of Clinical Medicine and Cardiovascular Research Center, National Yang-Ming University, Taipei, Taiwan.

[3]Department of Radiological Technology, Central Taiwan University of Science and Technology, Taichung, Taiwan.

[4]Cardiovascular Center, Taichung Veterans General Hospital, Taichung, Taiwan.

[5]Department of Orthopedic Surgery, China Medical University Hospital, Taichung, Taiwan.

**WEB**
This is a Web exclusive article.

*AJR* 2009; 192:W245–W254

0361–803X/09/1925–W245



For several years, MDCT has been widely used in many cardiovascular applications because of its robust spatial resolution. Many studies have confirmed the accuracy of MDCT in evaluating renal artery stenosis [1, 2]. Because its spatial resolution is superior to that of MRI and its acquisition time is shorter, MDCT is now widely used in clinical practice to survey patients with suspected renal hypertension except those contraindicated for iodinated contrast medium or ionizing radiation. Radiologists should evaluate not only the renal arteries but also the whole scanned region including the renal parenchyma and adrenal glands because important incidental findings of diseases that present as hypertension could be detected [3–5]. In this article, we will use many illustrations to review the concept of a comprehensive evaluation of patients with suspected renal hypertension using MDCT.

## Techniques

All of the patients described in this article were imaged using a 40-MDCT scanner (Brilliance 40, Philips Healthcare). Any MDCT scanner with submillimeter collimation could theoretically achieve the same results. The arterial phase scan included the region from the diaphragm to the iliac arteries [1, 2] to cover all the potential origins of the accessory renal arteries [6, 7] (Fig. 1). The thinnest collimation and reconstruction thickness (range, 0.5–0.75 mm, according to the type of scanner) should be used to provide detailed volumetric data.

A contrast medium volume of 1.3 mL/kg of body weight was injected intravenously and followed by a 30-mL saline chaser. No oral contrast medium was given. A bolus-tracking technique was used to synchronize scanning and contrast injection with a region of interest in the abdominal aorta. The flow rate was determined by the contrast-covering time concept to obtain high and homogeneous enhancement [8, 9]. For a detailed description of contrast-covering time, please refer to the associated references [8, 9]. The flow rate could be determined by the following equation:

$$\text{contrast volume / flow rate} = \frac{\text{postthreshold delay} + \text{scan time} + \text{safe margin}}{}$$

$$\text{Flow rate} = 1.3\ \text{mL/kg} \times \text{body weight} / (7\ \text{seconds} + \text{scan time} + 5\ \text{seconds}) = 1.3\ \text{mL/kg} \times \text{body weight} / (\text{scan time} + 12\ \text{seconds})$$

For parenchymal phase imaging, we used a low-dose protocol 4 minutes after contrast

injection (Fig. 1). The scan covered only the bilateral renal parenchyma. A low-kilovoltage technique was used to provide a lower radiation dose but maintain acceptable image quality [10]. For the radiation control of scanning for both phases, we adjusted the radiation parameters according to the abdominal lateral width at the kidney level (Fig. 1 and Table 1). The automatic online dose modulation option provided by the scanner was also turned on.

The reason for obtaining parenchymal phase images is to visualize parenchymal diseases that are reported to be related to hypertension, including renal cell carcinoma [11], renal stone [12], and renin-secreting tumor [3, 4]. Evaluation of the renal parenchyma is easier in the parenchymal phase because of homogeneous enhancement between the renal cortex and medulla.

In patients in whom renal hypertension is suspected, ischemic nephropathy might have already developed [13]; therefore, calculating the estimated glomerular filtration rate (GFR) before scanning is critically important to avoid renal failure. For patients with an estimated GFR of between 30 and 59 mL/min, especially those with other risk factors such as diabetes mellitus, isoosmolar contrast medium should be used to prevent contrast-induced acute kidney injury. For patients with an estimated GFR of less than 30 mL/min, nephrology consultation is suggested before scanning. If MDCT is still necessary, dialysis before and after the procedure is suggested [14].

Adjusting the radiation dose according to the patient's body habitus is a recent trend [15]. In patients with suspected renal artery stenosis, minimizing radiation dose is important because many of these patients are children or young women who are sensitive to radiation. Adjusting scanning parameters according to the patient's lateral width (Fig. 1) is based on the concept of the half-value layer [16]. The suggested radiation table was created and modified according to the recommendations of the American Association of Physicists in Medicine [16] and our clinical experience (Table 1). The tube current is displayed as milliampere-seconds per section to adjust for the pitch and rotation time to make it easier to apply in different scanners.

Because the renal arteries and adrenal glands are small structures with 3D configuration, we suggest that radiologists use a CT workstation that can interactively display any plane and thickness and that allows postprocessing techniques for interpretation. Axial thin- or thick-section images, maximum-intensity-projection techniques, and volume-rendering techniques should be used interchangeably and complementarily to provide a complete evaluation [17, 18] (Fig. 1).

**TABLE 1: Radiation Table With CT Parameters Adjusted According to Patient's Abdominal Lateral Width at the Level of the Kidneys**

| | Arterial Phase[a] | | | Delayed Phase[b] | | |
|---|---|---|---|---|---|---|
| Lateral Width (cm) | Tube Voltage (kV) | Effective mAs (mAs/slice) | $CTDI_{vol}$ (mGy) | Tube Voltage (kV) | Effective mAs (mAs/slice) | $CTDI_{vol}$ (mGy) |
| 20.0–21.9 | 120 | 85 | 6.0 | 80 | 170 | 3.6 |
| 22.0–23.9 | 120 | 95 | 6.7 | 80 | 190 | 4.1 |
| 24.0–25.9 | 120 | 105 | 7.4 | 80 | 210 | 4.5 |
| 26.0–27.9 | 120 | 115 | 8.5 | 80 | 230 | 4.9 |
| 28.0–29.9 | 120 | 125 | 8.8 | 80 | 250 | 5.4 |
| 30.0–31.9 | 120 | 150 | 10.5 | 80 | 300 | 6.4 |
| 32.0–33.9 | 120 | 175 | 12.3 | 80 | 350 | 7.5 |
| 34.0–35.9 | 120 | 200 | 14.0 | 80 | 400 | 8.6 |
| 36.0–37.9 | 120 | 225 | 15.8 | 80 | 450 | 9.6 |
| 38.0–39.9 | 120 | 250 | 17.5 | 80 | 500 | 10.7 |
| 40.0–41.9 | 120 | 300 | 21.0 | 120 | 185 | 12.9 |
| 42.0–43.9 | 120 | 350 | 24.5 | 120 | 215 | 15.0 |
| 44.0–45.9 | 120 | 400 | 28.0 | 120 | 245 | 17.1 |
| 46.0–47.9 | 140 | 305 | 31.5 | 120 | 275 | 19.3 |
| 48.0–49.9 | 140 | 335 | 35.0 | 120 | 310 | 21.4 |

Note—$CTDI_{vol}$ = volumetric CT dose index.
[a]Arterial phase was performed with a rotation time of 0.5 second, pitch of 0.676, slice thickness of 0.67 mm, and index of 0.33 mm.
[b]Delayed phase was performed with a rotation time of 1.0 second, pitch of 0.676, slice thickness of 0.8 mm, and index of 0.4 mm.

## Renal Artery Evaluation

### *Renal Artery Stenosis*

*Atherosclerosis*—Atherosclerosis is the most common cause of renal artery stenosis [13]. These stenoses are usually seen in the ostium or the proximal third of the renal arteries (Fig. 2). Plaque, which can be soft, calcified, or mixed in composition, is always observed. Because of MDCT's high spatial resolution, the plaque can be easily quantified to determine whether the patient should receive endovascular intervention. The criterion of "significant stenosis" varies in different studies and among institutions, reflecting controversy about the indications for endovascular revascularization [13]. Our criterion is that a stenosis of more than 70% of the artery's diameter should be considered for endovascular revascularization if the patient has a compatible clinical history [13].

*Fibromuscular dysplasia*—Fibromuscular dysplasia, the second most common cause for renal artery stenosis, is usually seen in young women (< 50 years old) [13]. The stenoses are usually found in the proximal or middle portion of the renal arteries (Fig. 3). A string-of-beads appearance, which indicates successive aneurysms and luminal stenoses, is the diagnostic feature. These patients are good candidates for endovascular intervention because of their excellent prognosis after the procedure [13]. MDCT is an important technique in identifying patients who will benefit from intervention [19].

*Follow-up after stenting*—After stent placement, MDCT can be a great follow-up tool [18] because it is probably the only noninvasive technique capable of directly visualizing the intrastent lumen with high spatial resolution (Fig. 4). These patients usually present with recurrent hypertension or decreased renal size after renal artery stenting.

### *Renal Artery Thromboembolism with Infarction*

In some patients, the rapid development of resistant hypertension presents with decreasing renal function and even flank pain [20]. These findings should raise the possi-

bility of acute thromboembolism. The extent of thromboembolism can be evaluated in the renal arteries (Fig. 5). The enhancement of the renal parenchyma can also be assessed to determine the viability of the kidneys [20] (Fig. 5). Because the disease is uncommon, there is no guideline for therapy. Several case series in the literature that used intraarterial local infusion of a thrombolytic agent achieved good results [21, 22].

## Facilitating Endovascular Intervention

MDCT can provide general information about the aorta, such as whether an abdominal aneurysm, a dissection, or ulcerative plaques are present that might complicate the interventional procedure for interventional radiologists and cardiologists. In addition, the following points should also be carefully checked.

### *Accessory Renal Arteries*

The accessory renal arteries have origins distant from both kidneys; sometimes they can even arise from the iliac arteries [6, 7]. The accessory arteries should be identified and completely evaluated because stenosis in these arteries can also cause renal hypertension (Fig. 6). If these arteries are not identified, the diagnosis could be delayed because sonography and catheter angiography are needed to localize these aberrant vessels.

### *Projection Angle*

With the inherent volumetric nature of MDCT, we can easily evaluate the best projection angle for visualization of any lesion while performing an endovascular intervention (Fig. 6). This capability is particularly useful when several stenoses and arteries need to be treated. In some institutions, MDCT is also used as a planning tool for protection devices; however, because the availability of renal protection devices is still limited, discussion is beyond the scope of this article.

## Findings Beyond Renal Arteries

### *Renin-Secreting Tumor*

Patients with renin-secreting tumor also present with resistant hypertension [3, 4]. These tumors are uncommon, with only eight cases per 30,000 hypertensive patients, and diagnosis is usually delayed because they are misdiagnosed as renal cysts or are even just overlooked (Fig. 7). These tumors are small and are easily obscured by heterogeneous enhancement in the arterial phase, emphasizing the importance of the delayed parenchymal phase. For young hypertensive patients with patent renal arteries and secondary hyperaldosteronism, renin-secreting tumor should be suspected if a complicated cyst or renal tumor is found on cross-sectional imaging techniques such as sonography, MDCT, or MRI [3, 4].

### *Adrenal Lesions*

Adrenal lesions—for example, pheochromocytoma, adrenal cortical hyperplasia (Fig. 8), and cortical adenoma—can also cause resistant hypertension [5]. Thus, a comprehensive evaluation of a patient with resistant hypertension should include the bilateral adrenal glands to see whether there are masses, nodules, or hypertrophy.

### *Renal Cell Carcinoma*

Resistant hypertension can be associated with renal cell carcinoma [11]. Some patients initially suspected of having renal artery stenosis later prove to have renal cell carcinoma (Fig. 9). The size, enhancement, and vessel invasion of the tumor can be correctly assessed by a combined reading of arterial and parenchymal phase images.

### *Renal Stone*

Renal stone formation is thought to be related to the microenvironment of the kidney [12]. Hypertension and renal stone formation have many common inducing factors [12]. Many patients who present with resistant hypertension are later found to have renal stones. Removing the stone and its local irritation sometimes relieves the hypertension.

### *Page Kidney*

After trauma or anticoagulant use, in some patients, a hematoma develops in the subcapsular region of the kidney. With the compression effect of the hematoma to the renal parenchyma, the renin–angiotensin–aldosterone system could be activated and present hypertension clinically. The condition is named "Page kidney" and can be diagnosed with a typical history and visualization of the subcapsular hematoma on MDCT [23].

## Comprehensive MDCT Reporting

In a comprehensive report, the following clinical questions should be answered: Is there a renal artery stenosis (Figs. 1–3)? How severe is the stenosis (Fig. 1)? Have the accessory renal arteries been identified and evaluated (Fig. 6)? What is the best projection angle with which to show the stenosis for endovascular intervention (Fig. 6)? Was the patient treated by stenting (Fig. 4)? If yes, was the intrastent lumen patent, restenosed, or occluded (Fig. 4)? Are there any other findings about the renal parenchyma (Figs. 5, 7, 9), adrenal glands (Fig. 8), or the abdomen (Fig. 2)? With this comprehensive approach, we can make the best use of the MDCT scans to provide important information to the clinician, the interventionist, and the patient.

## Conclusion

For the evaluation of patients with suspected renal hypertension, we can use MDCT to offer information about the renal arteries, renal and perirenal regions, and whole scanned abdomen. Radiologists should equip themselves with the knowledge to set the protocol, adjust the radiation dose, and interpret the MDCT scans comprehensively.

## References


1. Fraioli F, Catalano C, Bertoletti L, et al. Multidetector-row CT angiography of renal artery stenosis in 50 consecutive patients: prospective interobserver comparison with DSA [in English and Italian]. *Radiol Med* 2006; 111:459–468
2. Rountas C, Vlychou M, Vassiou K, et al. Imaging modalities for renal artery stenosis in suspected renovascular hypertension: prospective intraindividual comparison of color Doppler US, CT angiography, GD-enhanced MR angiography, and digital subtraction angiography. *Ren Fail* 2007; 29:295–302
3. Chung CT, Chen JW, Wu TR, et al. Secondary hypertension due to renin secreting tumor: a case report. *Zhonghua Yi Xue Za Zhi (Taipei)* 1994; 54:188–192
4. Haab F, Duclos JM, Guyenne T, et al. Renin secreting tumors: diagnosis, conservative surgical approach and long-term results. *J Urol* 1995; 153: 1781–1784
5. Capricchione A, Winer N, Sowers JR. Adrenocortical hypertension. *Curr Urol Rep* 2006; 7:73–79
6. Ozkan U, Oğuzkurt L, Tercan F, Kizilkiliç O, Koç Z, Koca N. Renal artery origins and variations: angiographic evaluation of 855 consecutive patients. *Diagn Interv Radiol* 2006; 12:183–186
7. Raman SS, Pojchamarnwiputh S, Muangsomboon K, Schulam PG, Gritsch HA, Lu DS. Utility of 16-MDCT angiography for comprehensive preoperative vascular evaluation of laparoscopic renal donors. *AJR* 2006; 186:1630–1638
8. Tsai WL, Tsai IC, Lee T, Hsieh CW. Polyarteritis nodosa: MDCT as a "one-stop shop" modality for whole-body arterial evaluation. *Cardiovasc Intervent Radiol* 2008; 31[suppl 2]:S26–S29
9. Tsai IC, Lee T, Chen MC, Tsai WL, Lin PC, Liao

WC. Homogeneous enhancement in pediatric thoracic CT aortography using a novel and reproducible method: contrast-covering time. *AJR* 2007; 188:1131–1137

10. Nakayama Y, Awai K, Funama Y, et al. Abdominal CT with low tube voltage: preliminary observations about radiation dose, contrast enhancement, image quality, and noise. *Radiology* 2005; 237:945–951
11. Wong PS, Lip GY, Gearty JC, et al. Renal cell carcinoma and malignant phase hypertension. *Blood Press* 2001; 10:16–21
12. Borghi L, Meschi T, Guerra A, et al. Essential arterial hypertension and stone disease. *Kidney Int* 1999; 55:2397–2406
13. Garovic VD, Textor SC. Renovascular hypertension and ischemic nephropathy. *Circulation* 2005; 112:1362–1374
14. McCullough PA. Contrast-induced acute kidney injury. *J Am Coll Cardiol* 2008; 51:1419–1428
15. Goske MJ, Applegate KE, Boylan J, et al. The "Image Gently" campaign: increasing CT radiation dose awareness through a national education and awareness program. *Pediatr Radiol* 2008; 38:265–269
16. McCollough C, Cody D, Edyvean S, et al.; Diagnostic Imaging Council CT Committee. The measurement, reporting, and management of radiation dose in CT. College Park, MD: American Association of Physicists in Medicine, January 2008: AAPM report no. 96
17. Saba L, Caddeo G, Sanfilippo R, Montisci R, Mallarini G. Multidetector-row CT angiography diagnostic sensitivity in evaluation of renal artery stenosis: comparison between multiple reconstruction techniques. *J Comput Assist Tomogr* 2007; 31:712–716x
18. Puchner S, Stadler A, Minar E, Lammer J, Bucek RA. Multidetector CT angiography in the follow-up of patients treated with renal artery stents: value of different reformation techniques compared with axial source images. *J Endovasc Ther* 2007; 14:387–394
19. Sabharwal R, Vladica P, Coleman P. Multidetector spiral CT renal angiography in the diagnosis of renal artery fibromuscular dysplasia. *Eur J Radiol* 2007; 61:520–527
20. Kawashima A, Sandler CM, Ernst RD, Tamm EP, Goldman SM, Fishman EK. CT evaluation of renovascular disease. *RadioGraphics* 2000; 20: 1321–1340
21. Cheng BC, Ko SF, Chuang FR, Lee CH, Chen JB, Hsu KT. Successful management of acute renal artery thromboembolism by intra-arterial thrombolytic therapy with recombinant tissue plasminogen activator. *Ren Fail* 2003; 25:665–670
22. Salam TA, Lumsden AB, Martin LG. Local infusion of fibrinolytic agents for acute renal artery thromboembolism: report of ten cases. *Ann Vasc Surg* 1993; 7:21–26
23. Haydar A, Bakri RS, Prime M, Goldsmith DJ. Page kidney: a review of the literature. *J Nephrol* 2003; 16:329–333

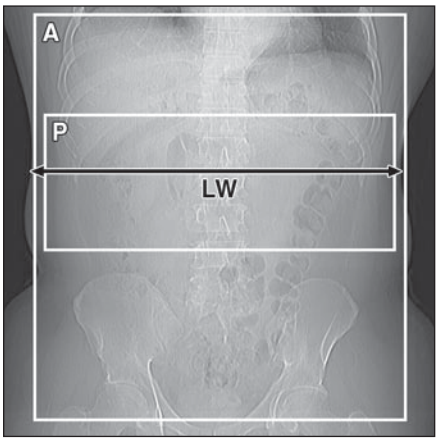


A

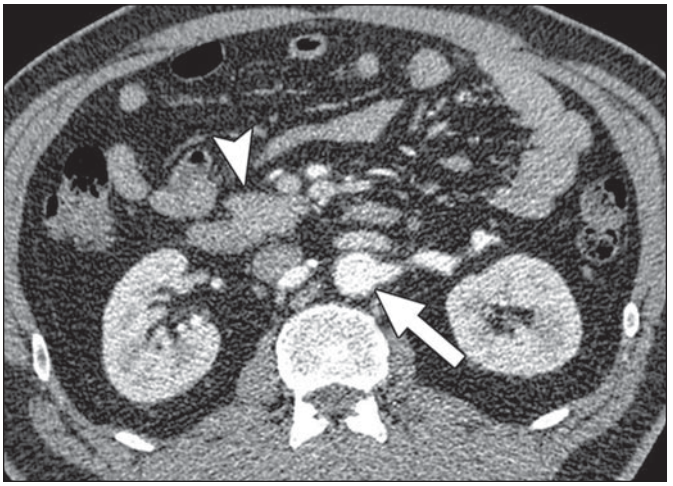

B

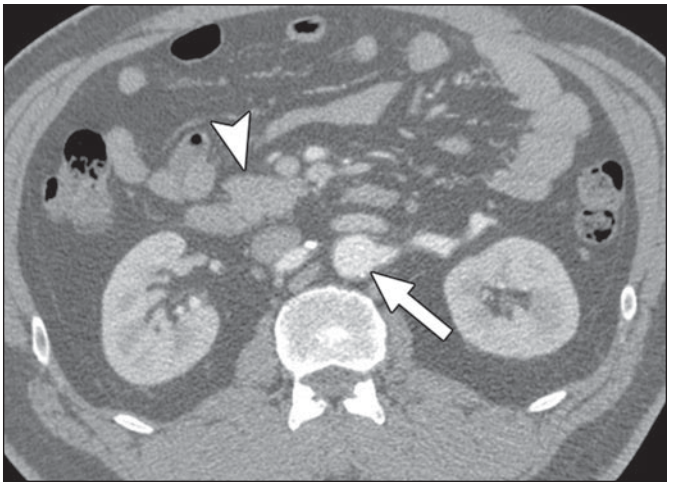

C

**Fig. 1**—46-year-old man with resistant hypertension who underwent renal artery stenosis survey. Body weight of patient was 100 kg. This case shows scanning protocol, image postprocessing, and interpretation algorithm.
**A,** Scout film of scan. After scout image is obtained, scan ranges of arterial phase (A) and parenchymal phase (P) are defined. Abdominal lateral width (LW) at kidney level is then measured to determine radiation parameters according to Table 1.
**B,** Axial thin-section (0.67-mm) image of arterial phase MDCT. Image is displayed in routine CT angiography window with center of 40 HU and width of 400 HU. Obvious image noise can be identified—for example, within aorta (*arrow*) and pancreatic head parenchyma (*arrowhead*). Noise level measured in aorta is 41 HU, which makes routine image interpretation difficult.
**C,** Axial thick-section (3-mm) image of arterial phase MDCT. When thickness is increased, noise is greatly reduced compared with **B**. Also, viewing image in wider window width (800 HU) further reduces perceived image noise. Radiologist could use this image setting to scroll up and down to evaluate whole abdomen. Note significantly decreased noise in aorta (*arrow*) and pancreatic head parenchyma (*arrowhead*) compared with **B**.
**(Fig. 1 continues on next page)**

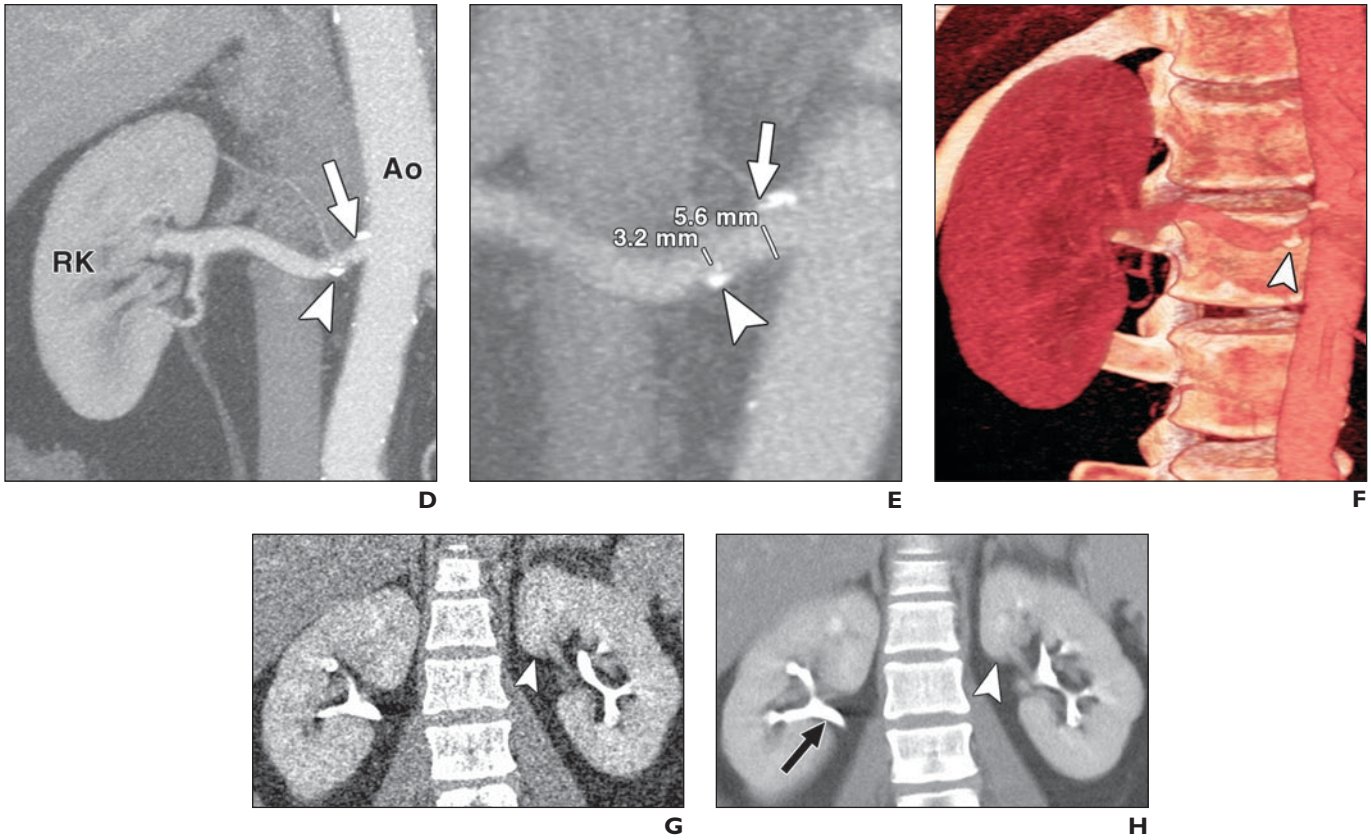


**Fig. 1 (continued)**—46-year-old man with resistant hypertension who underwent renal artery stenosis survey. Body weight of patient was 100 kg. This case shows scanning protocol, image postprocessing, and interpretation algorithm.
**D,** Oblique coronal image obtained for evaluation of right renal artery (*arrow*) with maximum-intensity-projection technique is then evaluated for any stenosis. Mixed plaque causing stenosis is noted over proximal right renal artery (*arrowhead*). Ao = aorta, RK = right kidney.
**E,** Zoomed oblique coronal image obtained for evaluation of proximal right renal artery stenosis lesion is used to quantify stenosis. Measuring most stenotic segment (*arrowhead*) and comparing it with proximal referenced vessel (*arrow*), we can quantify stenosis. In this case, stenotic segment is 3.2 mm in diameter and reference vessel is 5.6 mm in diameter, which creates stenosis of 43% [(5.6 mm – 3.2 mm) / 5.6 mm]. Endovascular revascularization is not indicated.
**F,** Oblique coronal slab volume-rendered image obtained for evaluation of right renal artery and right kidney. Volume-rendering technique provides good panoramic view, but it is not accurate in quantifying stenosis (*arrowhead*) because degree of stenosis is greatly affected by many parameters of volume-rendering technique such as opacity, threshold, and light source direction.
**G,** Coronal thin-section (0.8-mm) image of low-dose 4-minute parenchymal phase scan. Because of low-radiation technique, image noise is high (81.3 HU), which makes interpretation very difficult. Note noisy image in homogeneously enhanced renal parenchyma (*arrowhead*).
**H,** Coronal thick-section (8-mm) of low-dose 4-minute parenchymal phase scan. By increasing thickness, noise level dropped to 23.2 HU, which is good for clinical interpretation. Renal parenchyma (*arrowhead*) and collecting system (*arrow*) can be thoroughly evaluated. Note significantly decreased noise in renal parenchyma compared with **G**. Parenchymal phase imaging is good for detection of small tumors such as renin-secreting tumors.


A

B

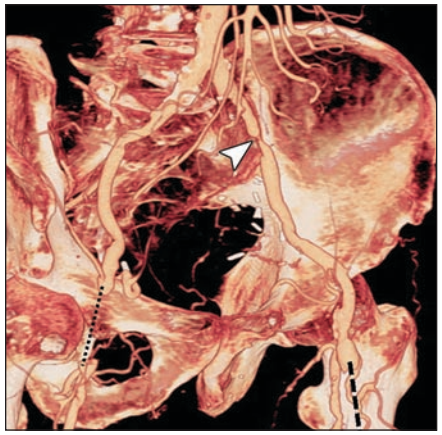

C

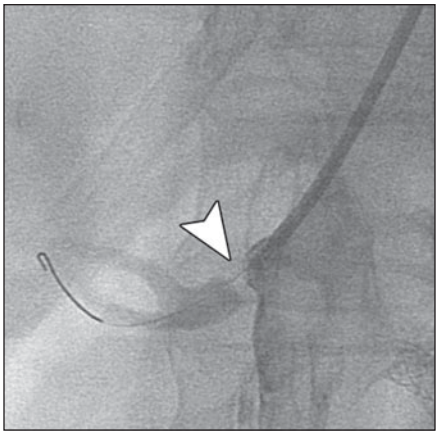

D

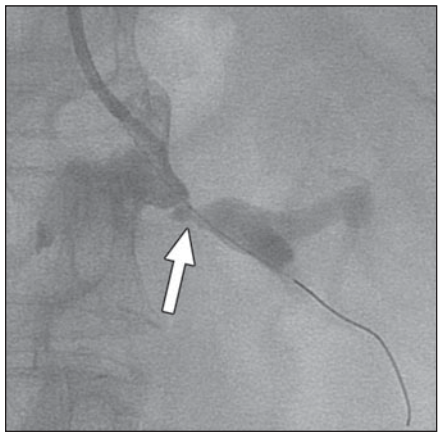

E

**Fig. 2**—73-year-old man diagnosed as having atherosclerotic bilateral renal artery stenoses who underwent endovascular treatment.
**A,** Coronal thin-section image shows right-side 90% (*arrowhead*) and left-side 70% (*arrow*) renal artery stenoses. In atherosclerotic renal artery stenosis, plaque can always be identified. In this case, right-side renal artery stenosis is caused by noncalcified plaque, and left-side renal artery is stenosed by mixed plaque. Ao = aorta.
**B,** Oblique sagittal slab volume-rendered image shows another critical stenosis over celiac ostium (*arrow*). Because atherosclerosis is systemic disease, multivessel involvement is common. All major arteries in scanned region must be evaluated to provide comprehensive report.
**C,** Oblique coronal volume-rendering image shows poor bilateral lower limb arterial conditions. Chronic total occlusion is noted over right common femoral artery (*dotted line*) and left superficial femoral artery (*dashed line*). Left external iliac artery also shows critical lesion (*arrowhead*). For endovascular intervention, femoral artery approach is thus not suggested. In report, interpreting radiologist suggested upper limb approach for renal artery intervention.
**D,** Anteroposterior view of catheter angiography shows right renal artery stenosis is so critical that stenotic lumen (*arrowhead*) is barely visible. Guidewire passage confirmed lesion was critically stenotic rather than chronically occluded. Also, note that catheter reaches renal artery via radial artery approach, as radiologist suggested in report.
**E,** Anteroposterior view of catheter angiography for left renal artery shows left renal artery stenosis of 70% (*arrow*). Both lesions in renal arteries were then treated by angioplasty and stenting.

**Fig. 3**—24-year-old woman with resistant hypertension due to fibromuscular dysplasia.
**A,** Oblique axial slab volume-rendered image. Viewing angle is from diaphragm to be able to see abdominal vessels, with patient's left side on left side of image. Both right-side (*arrowhead*) and left-side (*arrow*) renal artery stenoses can be clearly identified. Ao = aorta, CT = celiac trunk.
**B,** Axial maximum-intensity-projection image of right renal artery shows near total occlusion (*arrowhead*) over right proximal renal artery. Note stenosis is not caused by atherosclerosis; thus, no plaque can be seen.
**C,** Oblique coronal maximum-intensity-projection image of left renal artery shows critical lesion (*arrow*) over proximal left renal artery. Also, no plaque can be seen in this lesion.

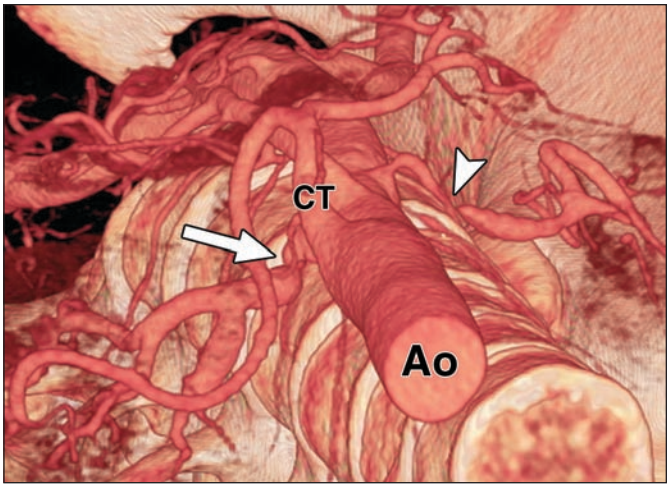


A

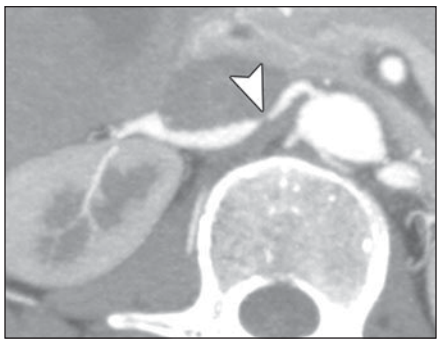

B

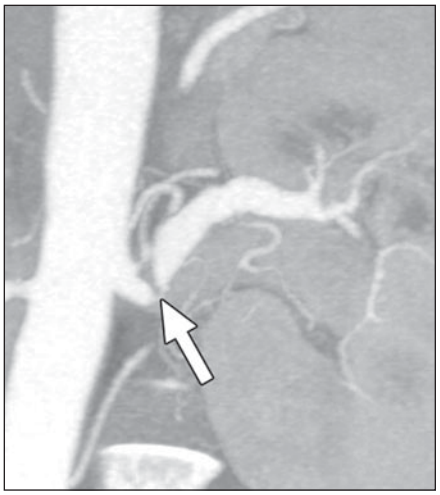

C

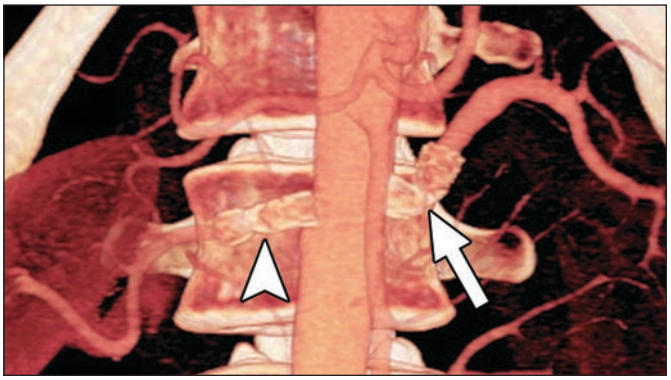

A

**Fig. 4**—24-year-old woman (same patient as in Figure 3) who underwent bilateral renal artery stenting for treatment of fibromuscular dysplasia.
**A,** Coronal slab volume-rendered image shows stent is placed over left (*arrow*) and right (*arrowhead*) proximal renal arteries. However, because of native vessel curvature, left renal artery stent shows angulation (*arrow*).

**(Fig. 4 continues on next page)**

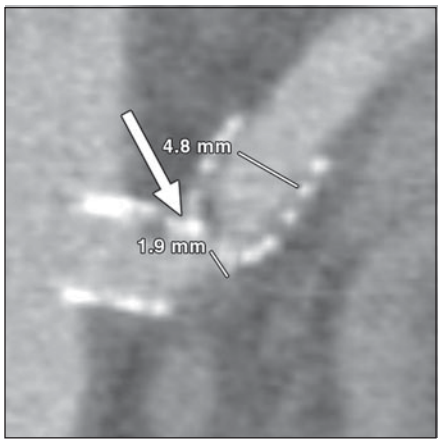


B

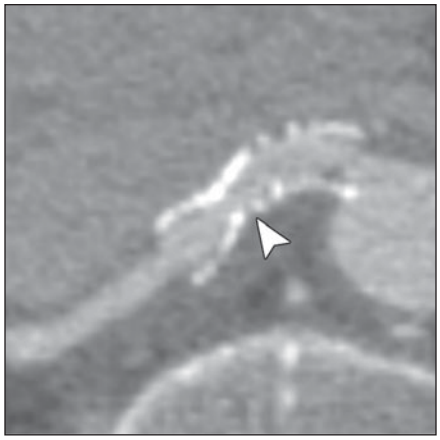

C

**Fig. 4 (continued)**—24-year-old woman (same patient as in Figure 3) who underwent bilateral renal artery stenting for treatment of fibromuscular dysplasia.
**B,** Thin-section oblique coronal image obtained for evaluation of left renal artery stent shows kink (*arrow*) over middle portion of stent with some intimal hyperplasia (thin black lining inside stent), but lumen is still patent.
**C,** Thin-section axial image obtained for evaluation of right renal artery stent shows patent intrastent lumen (*arrowhead*). Note that percutaneous transluminal renal artery angioplasty with stenting is standard treatment of fibromuscular dysplasia–associated renal hypertension. In most cases, stenting will result in good symptom relief.

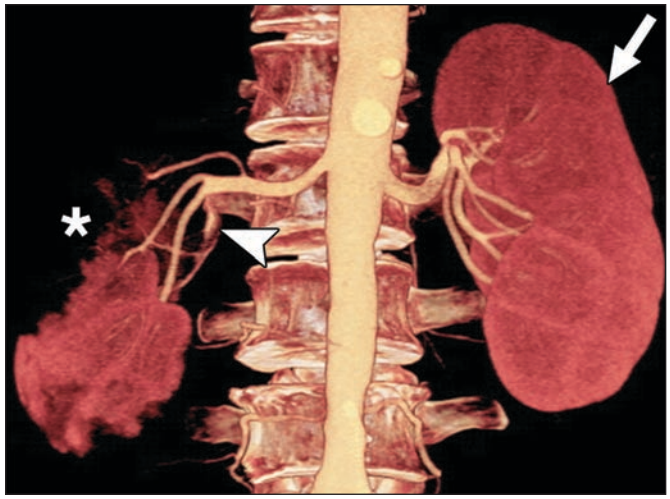

A

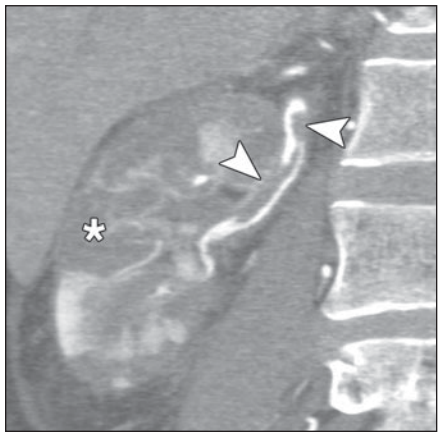

B

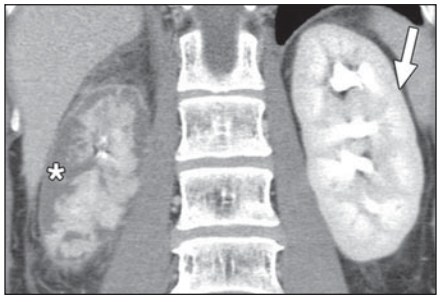

C

**Fig. 5**—48-year-old man who experienced right flank pain and resistant hypertension for 4 days and who was diagnosed as having right renal artery thromboembolism with renal infarction.
**A,** Coronal slab volume-rendered image shows long segment of filling defect over right renal artery (*arrowhead*) with poorly enhanced right kidney (*asterisk*) as compared with left kidney (*arrow*).
**B,** Coronal thin-section image obtained for evaluation of distal right renal artery and right kidney shows long segment of filling defect over right distal renal artery and poor enhancement over renal parenchyma particularly over renal cortex, which is more susceptible to ischemic injury. Right renal artery thromboembolism (*arrowheads*) with renal infarction (*asterisk*) was diagnosed.
**C,** Coronal image obtained for bilateral kidney comparison shows poorly enhanced right kidney with cortical necrosis (*asterisk*). Normal left kidney shows enhanced renal cortex (*arrow*), medulla, and collecting system.

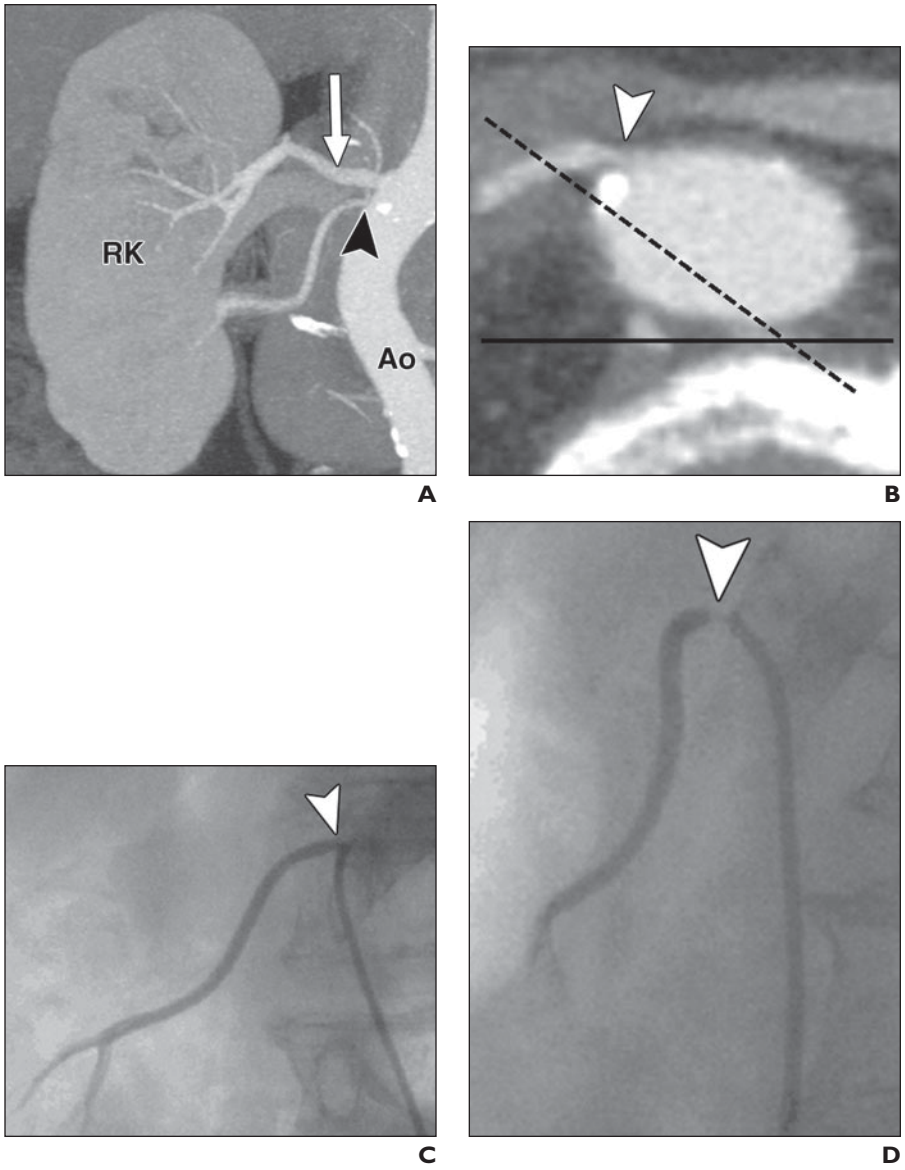


**Fig. 6**—83-year-old woman who was diagnosed with renal artery stenosis. This case shows importance of identifying accessory renal arteries and providing projection angle information.
**A,** Oblique coronal maximum-intensity-projection image obtained for evaluation of right renal arteries shows two renal arteries: Upper one is large (*arrow*) and lower one is smaller (*arrowhead*). If right lower renal artery, which has significant ostial stenosis, had not been identified, diagnosis and treatment might have been delayed. Ao = aorta, RK = right kidney.
**B,** Axial thin-section image obtained for evaluation of ostial stenosis of right inferior renal artery clearly shows stenosis (*arrowhead*). Best projection angle by which to approach lesion for catheter angiography is left anterior oblique 35° angle, which is shown by dashed line. Black solid line shows true anteroposterior projection.
**C,** True anteroposterior projection of catheter angiography for right renal artery injection cannot clearly show ostial lesion (*arrowhead*).
**D,** Left anterior oblique 35° projection of catheter angiography obtained for evaluation of right renal artery clearly shows ostial lesion (*arrowhead*). Interventionist might have overlooked ostial lesion if he or she had not been provided with projection angle information before procedure. Because of volumetric acquisition nature of MDCT, it is easy to find best projection angle for any renal stenotic lesion.

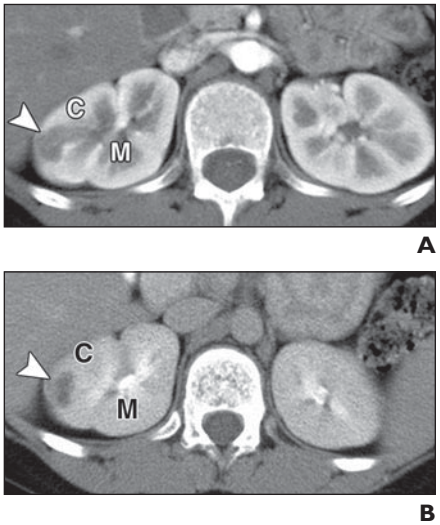


**Fig. 7**—10-year-old girl with elevated renin and resistant hypertension who was diagnosed as having renin-secreting tumor. C = cortex, M = medulla.
**A,** Axial image obtained in arterial phase shows poorly enhanced small nodule over right kidney (*arrowhead*). This tumor was initially misdiagnosed as prominent medulla or small renal cyst on arterial phase image by experienced radiologist. Note that in arterial phase, renal parenchyma enhancement is very heterogeneous, making evaluation of parenchyma difficult.
**B,** Axial image obtained in 4-minute parenchymal phase shows mild peripheral enhancement of tumor (*arrowhead*) that can be easily identified because of homogeneous enhancement of renal parenchyma. With percutaneous technique, lesion was confirmed to be renin-secreting tumor and was treated by cryotherapy. Resistant hypertension was then cured. Without parenchymal phase image, conclusion of MDCT study might have been "no renal artery stenosis," and diagnosis might have been delayed for years. This case illustrates importance of parenchymal phase scan for comprehensive evaluation.

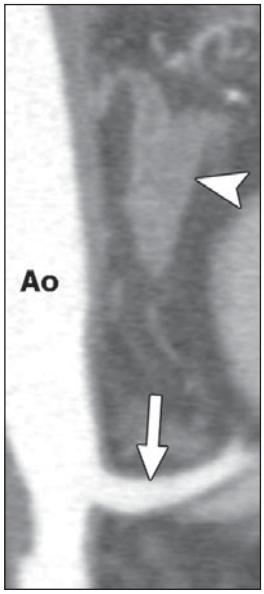


**Fig. 8**—69-year-old man who was diagnosed with resistant hypertension due to unilateral adrenal cortical hyperplasia. Oblique coronal image of left renal artery (*arrow*) and left adrenal gland (*arrowhead*) shows patent left renal artery and hypertrophied left adrenal gland, which is 10 mm in thickness. Left adrenal gland was then resected and resistant hypertension was cured. Ao = aorta.

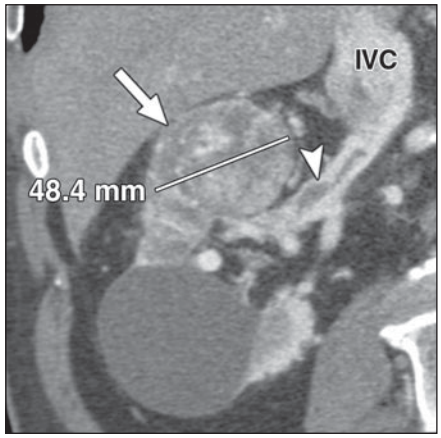


**Fig. 9**—78-year-old man who was initially suspected to have renal hypertension but was later diagnosed as having renal cell carcinoma. Oblique coronal image of right kidney and renal vein shows 48-mm mass lesion (*arrow*) over upper pole of right kidney with renal vein thrombosis (*arrowhead*), which is a typical finding for renal cell carcinoma. Right nephrectomy confirmed diagnosis. IVC = inferior vena cava.